A POSTERIORI STUDY OF FILTERED EULER-EULER TWO-PHASE MODEL USING A HIGH RESOLUTION SIMULATION OF A 3-D PERIODIC CIRCULATING FLUIDIZED BED

Ali Ozel, Pascal Fede, Olivier Simonin,
Institut de Mécanique des Fluides de Toulouse, Toulouse, France

Introduction

Gas-particle flows in vertical risers are involved in many industrial scale fluidized bed applications such as catalytic cracking, fossil or biomass combustion. Risers flows are often simulated by two-fluid model equations coupled with closures developed in the frame the kinetic theory of granular media (1–4). However, two-fluid model discretized over coarse mesh with respect to particle clustering size are performed for large units because of limited computational resources (5, 6). Now, it is well established that meso-scales cancelled out by coarse mesh simulations have dramatic effect on overall behaviour of flows (6–9).

Several attempts of the extension of two-fluid model by accounting for these unresolved structures have been done for coarse mesh simulations through different ways (6). In the framework of the filtered two-fluid model, Sundaresan and co-workers (7) performed highly resolved simulations of kinetic theory based two-fluid model equations for gas-particle flow in 2-D and 3-D periodic domain and it was stated that the existence of meso-scale structures causes overestimation of the drag force and underestimation of the particle agitation production and dissipation. Following this study, (10) proposed an ad-hoc sub-grid models for effective drag force and particle stresses which accounts for the effects of unresolved structures on the resolved flows. (8, 11) presented a filtering approach methodology to construct closures for the effective drag force and the effective particle stresses. (9) proposed an effective drag model dependent on the filter size and the solid volume fraction for 2-D bubbling fluidized bed.

Such high resolutions simulations using the standard two-fluid model (1, 2) were performed by (12) for a 3-D periodic circulating fluidized bed (PCFB) where typical FCC particles ($d_p = 75\,\mu m$, $\rho_p = 1500\,kg/m^3$) were interacting with the ambient gas ($\rho_g = 1.186\,kg/m^3, \mu_g = 1.8 \times 10^{-5}\,Pa.s$). The mean gas-solid flow were periodically driven along the opposite direction of gravity and concerning the transfers between the phases with non-reactive isothermal flow, the drag and buoyancy forces were accounted for the momentum transfer. The effect of the fluctuations of the gas velocity at small scales was neglected. The computational domain is shown in Figure 1. (12) refined computational grids to get mesh-independent result in which statistical quantities do not change with any further mesh refinement. Instantaneous particle volume fraction fields in the periodic circulating fluidized bed for different mesh resolutions are shown in Figure 2. This result were then filtered by volume averaging and used to perform a priori analyses on the filtered phase balance equations. Consistent results with previous studies were obtained. The physical identification of over-prediction of drag force was determined and these results show that filtered momentum equation could be computed on coarse grid simulation but must take into account the particle to fluid drift velocity (sub-grid drift velocity) due to the sub-grid correlation between the local fluid velocity and the local particle volume fraction (9, 12, 13). Closure relation is needed for the sub-grid drift velocity and several models were proposed, herein, we discuss only the Functional model (see (12) for other models). Additionally, (12) proposed to use the Yoshizawa model (14) for the trace of particle sub-grid stress tensor and the standard compressible Smagorinsky model (15) as in the single phase flows for the anisotropic parts of stresses.

The objective of the present study is to verify these models in posteriori studies. For posteriori studies, mesh independent of a 3-D PCFB was used as a reference for making comparisons. The numerical simulations have been carried out using an unsteady Eulerian multi-fluid approach implemented in the unstructured parallelized code NEPTUNE_CFD V1.07@Tlse. NEPTUNE_CFD is a multiphase flow software developed in the framework of the NEPTUNE project, financially supported by CEA (Commissariat à l'Energie Atomique), EDF (Electricité De France), IRSN (Institut de Radioprotection et de Sûreté Nucléaire) and AREVA-NP.

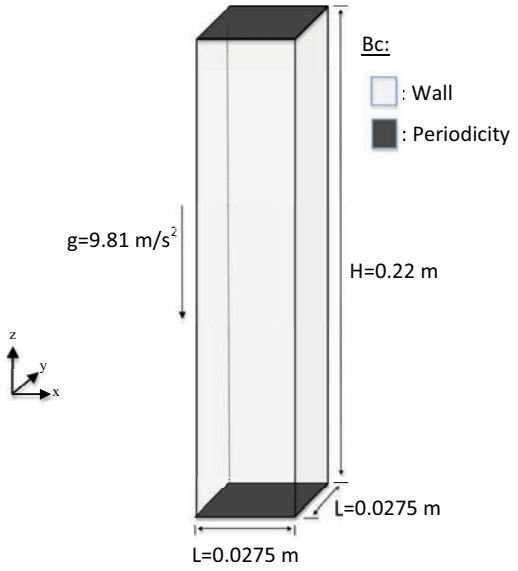

Figure 1: The periodic circulating fluidized bed (PCFB).

Figure 2: Instantaneous particle volume fraction field in the periodic circulating fluidized bed for different mesh resolutions. From right to left, the mesh resolution increases. White color corresponds to $\alpha_p = 0$. Black color corresponds to $\alpha_{p,max} = 0.64$.

Particulate Sub-grid Models

Functional Model

The proposed model for the effective drag term is given by

$$\overline{\frac{\alpha_p \rho_p}{\tau_p} V_{r,\beta}} = \frac{\rho_p}{\widetilde{\tau}_p} \left[1 + K_{\beta\beta} h(\overline{\alpha}_p) f(\overline{\Delta}^*)\right] \overline{\alpha}_p \left(\widetilde{U}_{g,\beta} - \widetilde{U}_{p,\beta}\right) \tag{1}$$

where the subscript β is used to indicate that there is no implicit summation, $K_{\beta\beta}$ is the model constant, $h(\overline{\alpha}_p)$ and $f(\overline{\Delta}^*)$ are two independent functions. $h(\overline{\alpha}_p)$ is the solid volume fraction dependency of the model and the following suggested form of this function is obtained from high resolution PCFB simulation:

$$h(\overline{\alpha}_p) = -tanh\left(\frac{\overline{\alpha}_p}{C_{h,1}}\right)\sqrt{\frac{\overline{\alpha}_p}{\alpha_{p,max}}}\left(1-\frac{\overline{\alpha}_p}{\alpha_{p,max}}\right)^2 \left(1-C_{h,2}\frac{\overline{\alpha}_p}{\alpha_{p,max}}+C_{h,3}\left(\frac{\overline{\alpha}_p}{\alpha_{p,max}}\right)^2\right) \tag{2}$$

with constants $C_{h,1}$, $C_{h,2}$ and $C_{h,3}$ 0.1, 1.88, 5.16, respectively. The maximum volume fraction of solid phase $\alpha_{p,max}$ is set to 0.64. The dependence of model on the filter width is given by:

$$f(\overline{\Delta}^*) = \frac{\overline{\Delta}^{*2}}{C_{f,1}+\overline{\Delta}^{*2}} \tag{3}$$

with the constant $C_{f,1}$ equal to 0.15 and $\overline{\Delta}^*$ is given by

$$\overline{\Delta}^* = \frac{\overline{\Delta}}{\tilde{\tau}_p\,|\tilde{\mathbf{V}}_r|} \tag{4}$$

where $\tilde{\tau}_p$ is the filtered relaxation time, $|\tilde{\mathbf{V}}_r|$ is the magnitude of the filtered relative velocity and $\overline{\Delta}$ is the filter width. The constant $K_{\beta\beta}$ is dynamically calculated and averaged over the domain to avoid numerical instabilities (12).

SGS Particle Stress Models

The particle sub-grid stress tensor $\sigma^{sgs}_{p,ij}$ can be decomposed into deviatoric and spherical parts. (15) model can be proposed for the anisotropic parts of stresses and (14) model can be used for the trace of stress tensor as follows:

$$\sigma^{sgs}_{p,ij} = \sigma^*_{p,ij} + \frac{1}{3}\sigma_{p,kk}\delta_{ij} \tag{5}$$

$$= -C_s^2\overline{\Delta}^2|\tilde{S}^*_p|\tilde{S}^*_{p,ij} + C_Y\overline{\Delta}^2|\tilde{S}^*_p|^2\delta_{ij} \tag{6}$$

with $\tilde{S}^*_{p,ij}$ the trace free strain rate tensor of the filtered particle velocity and given by

$$\tilde{S}^*_{p,ij} = \frac{\partial\tilde{U}_{p,i}}{\partial x_j} + \frac{\partial\tilde{U}_{p,j}}{\partial x_i} - \frac{2}{3}\frac{\partial\tilde{U}_{p,k}}{\partial x_k}\delta_{ij}. \tag{7}$$

$|\tilde{S}^*_p|$ is the norm of $\tilde{S}^*_{p,ij}$ and defined by $|\tilde{S}^*_p|^2 = 1/2\tilde{S}^*_{p,ij}\tilde{S}^*_{p,ij}$. The constants C_s and C_y are dynamically calculated by performing domain averaging along the mean flow (16).

Results and Discussions

Global Quantities

To investigate the dynamic behaviour of particles in the PCFB, (12) defined the statistic quantities averaged over domain and in time such as; particle agitation, relative velocity weighted by solid volume fraction and volumetric solid flux along the mean flow direction (see (12) for the procedure to calculate domain statistics for different mesh resolutions). Here, we discuss only the averaged volumetric solid flux obtained by the standard two-fluid model (TFM) and filtered-two fluid model (LES-TFM;

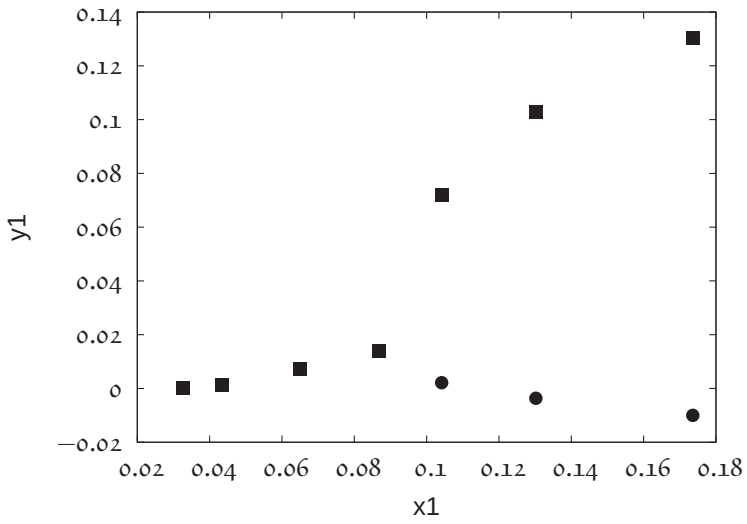

Figure 3: The influence of mesh size the non-dimensional total volumetric mass flux , $\overline{< G_s >}^t$ where $G_{s,o}$ corresponds to the homogeneous case and $G_{s,conv}$ corresponds to the converged case. ■: TFM simulations. ●; LES-TFM simulations for three mesh resolutions: coarse ($24 \times 24 \times 192$, $Fr_\Delta^{-1} = 0.175$), moderate ($32 \times 32 \times 256$, $Fr_\Delta^{-1} = 0.128$) and fine ($40 \times 40 \times 320$, $Fr_\Delta^{-1} = 0.104$).

the Functional model for the effective drag model and the Yoshizawa+Smagorinsky models for the effective particle stresses). The coarsest mesh resolution composed of $110\,000$ cells ($24 \times 24 \times 192$, $\Delta x = \Delta y = \Delta z = 1.145 \times 10^{-3}\, m$ with inverse Froude number, $Fr_\Delta^{-1} = 0.175$). The highest mesh resolution case consists of approximately 17 million cells ($128 \times 128 \times 1024$, $\Delta x = \Delta y = \Delta z = 0.215 \times 10^{-3}\, m$ with inverse Froude number, $Fr_\Delta^{-1} = 0.032$). The inverse Froude number Fr_Δ^{-1} based on the mesh size is given by

$$Fr_\Delta^{-1} = \frac{(\Delta x \Delta y \Delta z)^{1/3}}{(\tau_p^{St})^2 \, ||\mathbf{g}||} \tag{8}$$

with Stoke's relaxation time τ_p^{St} given by $\frac{\rho_p}{\rho_g} \frac{d_p^2}{18\nu_g}$ and $||\mathbf{g}||$ is the norm of the gravity acceleration. The characteristic length scale $(\tau_p^{St})^2 \, ||\mathbf{g}||$ was set to $0.0066\, m$. For LES-TFM simulations, the filter width is given by $\Delta = (\Delta x \Delta y \Delta z)^{1/3}$.

The non-dimensional solid fluxes obtained from LES-TFM simulations for three mesh resolutions: coarse ($24 \times 24 \times 192$, $Fr_\Delta^{-1} = 0.175$), moderate ($32 \times 32 \times 256$, $Fr_\Delta^{-1} = 0.128$), fine ($40 \times 40 \times 320$, $Fr_\Delta^{-1} = 0.104$) and mesh dependency study of non-dimensional fluxes obtained from TFM simulations are shown in Figure 3. Solid fluxes were predicted very well by LES-TFM simulations. However, there is slight mesh dependency of the proposed models. The time-domain averaged of models' constants $K_{\beta\beta}$, C_s and C_y for coarse, moderate and fine mesh resolutions are given in Table 1. Instantaneous solid volume fraction in PCFB obtained from TFM simulations for different mesh

Table 1: Time-averaged of models' constants $K_{\beta\beta}$, (where $\beta = x, y, z$), C_s and C_y for coarse, moderate and fine mesh resolutions.

Fr_Δ^{-1}	$\overline{< K_{xx} >}^t, \overline{< K_{yy} >}^t$	$\overline{< K_{zz} >}^t$	$\overline{< C_s >}^t$	$\overline{< C_y >}^t$
0.175	5.23	4.86	0.010	0.044
0.128	5.10	4.92	0.014	0.043
0.104	4.82	4.96	0.007	0.038

resolutions; $Fr_\Delta^{-1} = 0.128$ and $Fr_\Delta^{-1} = 0.032$ are shown in Figure 4. Coarse mesh simulation with

Figure 4: Instantaneous of solid volume fraction in the PCFB. White color corresponds to $\alpha_p = 0$. Black color corresponds to $\alpha_{p,max} = 0.64$. left: TFM with mesh resolution, $Fr_{\Delta}^{-1} = 0.032$ $(128 \times 128 \times 1024)$, centre: TFM with mesh resolution, $Fr_{\Delta}^{-1} = 0.128$ $(32 \times 32 \times 256)$, right: LES-TFM with mesh resolution, $Fr_{\Delta}^{-1} = 0.128$ $(32 \times 32 \times 256)$.

$Fr_{\Delta}^{-1} = 0.128$ can not predict segregation along the center-line in the PFCB. In this figure, coarse mesh simulations with $Fr_{\Delta}^{-1} = 0.128$ by LES-TFM are also shown. The LES-TFM simulation is capable to capture segregation of particles along the centre line even for coarse mesh simulation.

Conclusion

In this study, we performed Euler-Euler two-phase model simulations by using the effective drag force and the effective sub-grid stresses models for gas-solid flow in a 3-D periodic circulating fluidized bed over relatively coarse mesh with respect to the particle clustering size. The results show that the overall hydrodynamic behaviour is accurately predicted as comparing with mesh independent result of the same flow configuration. Further step is to perform simulations by using proposed and available models in the literature (e.g. (8, 11) and (9)) for the industrial-scaled fluidized bed application, make comparisons between models' predictions and validations with available experimental data.

Acknowledgements

This work was performed using HPC resources from GENCI-CINES (Grant 2012-x2012026012).

References

1. G. Balzer, A. Boëlle, and O. Simonin. Eulerian gas-solid flow modelling of dense fluidized bed. In *FLUIDIZATION VIII, Proc. International Symposium of the Engineering Foundation*, pages 409–418, 1995.

2. A. Gobin, H. Neau, O. Simonin, J.-R. Llinas, V. Reiling, and J.-L. Selo. Fluid dynamic numerical simulation of a gas phase polymerization reactor. *International Journal for Numerical Methods in Fluids*, 43(10-11):1199–1220, 2003.

3. D. Gidaspow, J. Jung, and R. K. Singh. Hydrodynamics of fluidization using kinetic theory: an emerging paradigm: 2002 Flour-Daniel lecture. *Powder Technology*, 148(2-3):123–141, 2004.

4. M.A. van der Hoef, M. van Sint Annaland, N.G. Deen, and J.A.M. Kuipers. Numerical simulation of dense gas-solid fluidized beds: a multiscale modeling strategy. *Annual Review of Fluid Mechanics*, 40(1):47–70, 2008.

5. S. Sundaresan. Modeling the hydrodynamics of multiphase flow reactors: Current status and challenges. *AIChE Journal*, 46(6):1102–1105, 2000.

6. J. Wang. A review of eulerian simulation of geldart A particles in gas-fluidized beds. *Industrial Engineering Chemistry Research*, 48(12):5567–5577, 2009.

7. K. Agrawal, P.N. Loezos, M. Syamlal, and S. Sundaresan. The role of meso-scale structures in rapid gas–solid flows. *Journal of Fluid Mechanics*, 445:151–185, 2001.

8. Y. Igci, A. T. Andrews, S. Sundaresan, S. Pannala, and T. O'Brien. Filtered two-fluid models for fluidized gas-particle suspensions. *AIChE Journal*, 54(6):1431–1448, 2008.

9. J.-F. Parmentier, O. Simonin, and O. Delsart. A functional subgrid drift velocity model for filtered drag prediction in dense fluidized bed. *AIChE Journal*, 58(4):1084–1098, 2012.

10. A.T. IV Andrews, P. N. Loezos, and S. Sundaresan. Coarse-grid simulation of gas-particle flows in vertical risers. *Industrial Engineering Chemistry Research*, 44(16):6022–6037, 2005.

11. Y. Igci and S. Sundaresan. Constitutive models for filtered Two-Fluid models of fluidized Gas–Particle flows. *Industrial & Engineering Chemistry Research*, 0(0), 10.1021/ie200190q.

12. A. Ozel. *Development of Large Eddy Simulation Approach for Simulation of Circulating Fluidized Beds*. PhD thesis, Université de Toulouse, Toulouse, France, 2011.

13. A. Ozel, J.-F. Parmentier, O. Simonin, and P. Fede. A priori test of effective drag modeling for filtered two-fluid model simulation of circulating and dense gas-solid fluidized beds. In *7th International Conference on Multiphase Flow - ICMF 2010 Proceedings*. International Conference on Multiphase Flow (ICMF), 2010.

14. A. Yoshizawa. Statistical theory for compressible turbulent shear flows, with the application to subgrid modeling. *Physics of Fluids*, 29(7):2152, 1986.

15. J. Smagorinsky. General circulation experiments with the primitive equations. *Monthly Weather Review*, 91(3):99–164, March 1963.

16. M. Germano, U. Piomelli, P. Moin, and W.H. Cabot. A dynamic subgrid-scale eddy viscosity model. *Physics of Fluids A: Fluid Dynamics*, 3(7):1760, 1991.